Simulation design of P–I–N-type all-perovskite solar cells with high efficiency*

Hui-Jing Du(杜会静)†, Wei-Chao Wang(王韦超), and Yi-Fan Gu(顾一帆)

College of Science, Yanshan University, Qinhuangdao 066004, *China*

(Received 26 September 2016; revised manuscript received 1 November 2016; published online 10 January 2017)

According to the good charge transporting property of perovskite, we design and simulate a p–i–n-type all-perovskite solar cell by using one-dimensional device simulator. The perovskite charge transporting layers and the perovskite absorber constitute the all-perovskite cell. By modulating the cell parameters, such as layer thickness values, doping concentrations and energy bands of n-, i-, and p-type perovskite layers, the all-perovskite solar cell obtains a high power conversion efficiency of 25.84%. The band matched cell shows appreciably improved performance with widen absorption spectrum and lowered recombination rate, so weobtain a high J_{sc} of 32.47 mA/cm^2. The small series resistance of the all-perovskite solar cell also benefits the high J_{sc}. The simulation provides a novel thought of designing perovskite solar cells with simple producing process, low production cost and high efficient structure to solve the energy problem.

Keywords: all-perovskite solar cells, device simulation, band matching, photovoltaic performance

PACS: 88.40.H–, 88.40.hj, 88.40.fc **DOI:** 10.1088/1674-1056/26/2/028803

1. Introduction

As a novel third-generation solar cell, perovskite solar cell (PSC) has caused a boom in scientific research with the significant enhancement of the power conversion efficiency (PCE) from 3.8% in 2009[1] to 22.1% in 2016.[2] Simpler planar configuration has been often chosen as the PSC structure in comparison with nanoporous scaffold samples. The planar PSC commonly possesses a heterojunction architectures with three main layers, i.e., electron transport material (ETM), perovskite absorber and hole transport material (HTM). The widely used ETM and HTM are TiO_2 and spiro-OMeTAD, respectively. However, the high temperature calcination of the TiO_2 layer and the relatively expensive spiro-OMeTAD affect the future commercialization of the PSCs. Although many alternatives have been used, the efficiency of the most novel cells still lag those with TiO_2 as ETM and spiro-OMeTAD as HTM.[3–5] Some high efficiency PSC devices use organic materials as ETM and HTM,[6] but the shortcomings of the organic materials, such as the poor crystallinity and stability, must be faced.

The fabricating process of the conventional PSCs with ETM and HTM made of different material systems is incompatible with mass and rapid fabrication. Although the simplified PSCs with neither HTM nor ETM have been obtained, their efficiencies are still low because of the poor contact with the electrodes. Researches show that the perovskites have strong absorption coefficients,[7] long charges diffusion lengths,[8,9] and excellent charge transfer properties.[10] Their charge transfer properties each have an ambipolar characteristic which shows the balanced transport lengths l_n and l_p for the electron and hole. While in the bulk heterojunction solar cells, the l_n and l_p differ by orders of magnitude.[11] Perovskite films with big crystals and few pinholes are necessary for their excellent charge transfer properties of the perovskite. The stability of the PSC has been enhanced by the improving the fabrication and encapsulation process.

Considering the excellent characteristics of the perovskite and the necessity of mass and low cost production of PSCs, we propose the all-perovskite solar cell designation similar to the all-silicon cells. Hetero-junction with intrinsic thin-layer (HIT) silicon solar cells have relatively high efficiency with p–i–n structure,[12] but there are neither theoretical reports nor experimental reports on all-perovskite solar cells. $CH_3NH_3PbI_3$ can be either n- or p-doped by changing the precursor ratio or thermal annealing. The carrier concentration can also vary by six orders of magnitude.[13] These results offer the potential possibility to fabricate all-perovskite solar cells with commercially scalable, fast, low-cost process, which can open new synthesis routes aside the conventional heterojunction devices. It is worth studying all-perovskite solar cells through simulation process. Much information about the defect, band offset and other cell parameters of the PSCs has been obtained based on semiconductor device principles.[14–16] The simulation can provide a novel thought of designing simpler and more efficient perovskite solar cells structure.

*Project supported by the Graduate Student Education Teaching Reform Project, China (Grant No. JG201512) and the Young Teachers Research Project of Yanshan University, China (Grant No. 13LGB028).

†Corresponding author. E-mail: hjdu@ysu.edu.cn

© 2017 Chinese Physical Society and IOP Publishing Ltd

2. Device architecture and simulation parameters

The device simulator SCAPS (version 3.3.02) is used as simulation platform. The perovskite solar cell employs planar architecture with layer configuration of glass substrate/TCO /n-type doping $CH_3NH_3PbI_3$ layer (ETM)/i-type $CH_3NH_3PbI_3$ (absorption layer)/p-type doping $CH_3NH_3PbI_3$ layer (HTM)/metal back contact (see Fig. 1). The n-type and p-type doped perovskite take the place of TiO_2 (ETM) and spiro-OMeTAD (HTM), respectively. The initial parameters set for device simulation selected from those reported theoretical and experimental researches[14–16] are summarized in Table 1. Other parameters not included in Table 1 are those that are the same as those in our previous literature.[17] Defect layers are inserted in the interface between the layers (p/i and i/n layer) to simulate a more realistic perovskite region with a large number of defects.[16]

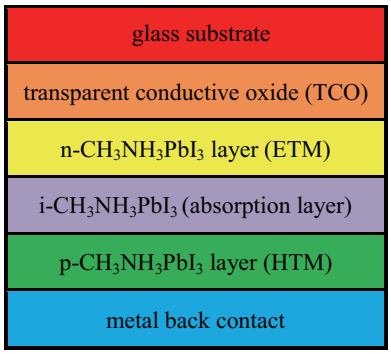


Fig. 1. (color online) Schematic diagram of the p–i–n-type all-perovskite solar cell.

Table 1. Simulation parameters of perovskite solar cells in this study.

Parameters	TCO	n-$CH_3NH_3PbI_3$	Defect layer	$CH_3NH_3PbI_3$ (absorber)	p-$CH_3NH_3PbI_3$
Thickness/nm	500	10 (variable)	10	300 (variable)	100 (variable)
Band gap energy E_g/eV	3.5	1.55 (variable)	1.55	1.55 (variable)	1.55 (variable)
Electron affinity χ/eV	4	3.9	3.9	3.9	3.9
Relative permittivity ε_r	9	6.5	6.5	6.5	6.5
Electron mobility μ_n/(cm^2·V·s)	20	2	2	2	2
Hole mobility μ_p/(cm^2·V·s)	10	2	2	2	2
Donor doping concentration N_D/cm^{-3}	2.00×10^{19}	1.00×10^{18} (variable)	1.00×10^{13}	1.00×10^{13}	0
Acceptor doping concentration N_A/cm^{-3}	0	0	0	0	1.00×10^{18} (variable)
Defect density N_t/cm^{-3}	1.00×10^{15}	2.50×10^{13}	1×10^{17}	2.50×10^{13}	2.50×10^{13}

In Section 3, according to the parameters set above, we investigate the photovoltaic property of the cell by adjusting the parameters of the cell, such as the thickness values, doping concentrations, and energy band E_g values of n-, i-, and p-type perovskite layers to obtain high power conversion efficiency. The control variable method is used during the parameter optimization, and the detailed simulation theory has been described in our previous papers.[17,18] Table 2 shows the simulation parameters and the cell performances in the three optimization processes: doping, thickness and band gap optimization. The cell performance is evidently improved by about 8.8% of the efficiency from the initial 17.05% to the final 25.843%. We believe that higher PCE can be obtained by further optimizing other parameters of the cell.

Table 2. Simulation parameters and the cell performance during the optimization.

	Parameters of the n, i, p layers			Cell performance			
	Thickness/nm	Doping concentration/cm^{-3}	Band gap energy E_g/eV	V_{oc}/V	J_{sc}/(mA/cm^2)	FF/%	E_{ff}/%
Initial cell	10, 300, 100	1.00×10^{18}, 1.00×10^{13}, 1.00×10^{18}	1.55, 1.55, 1.55	1.046	21.116	77.922	17.205
Doping optimization	10, 300, 100	3.00×10^{19} 1.00×10^{13}, 3.00×10^{19} (variable)	1.55, 1.55, 1.55	1.065	21.581	81.289	18.686
Thickness optimization	5, 500, 1000 (variable)	3.00×10^{19}, 1.00×10^{13}, 3.00×10^{19}	1.55, 1.55, 1.55	1.064	23.762	81.181	20.533
E_g optimization	5, 500, 1000	3.00×10^{19}, 1.00×10^{13}, 3.00×10^{19}	3.38, 1.4, 1.3 (variable)	0.956	32.474	83.278	25.843

3. Results and discussion

3.1. Influences of doping concentration of n-, p-layer perovskite

Doping is a very important process used to improve the properties of semiconductors devices, such as photovoltaic and light-emitting devices.[19,20] In silicon-based solar cells, appropriate p- or n-type doping is controlled accurately to achieve suitable energy position and carrier transport feature. The composition manipulations of the Cu (In, Ga)Se_2 solar cell can realize suitable self-doping and avoid deep defects.[19] In the light-emitting diode (LED) device, the carrier types and densities of the active and confining regions are adjusted to enhance the internal quantum efficiency.[20] Increasing conductivity of the HTM by doping could bring a positive influence on PCE of the planar heterojunction-based solar cells.[21,22] The experiments show that an appropriate doping in the perovskite can maximize the device efficiency.[23] Experimental researches[13,24] about the p and n self-doping in $CH_3NH_3PbI_3$ show that the carrier type, density, and charge transport in $CH_3NH_3PbI_3$ can be manipulated by changing the precursors ratio or thermal annealing. MAI-rich and PbI_2-rich perovskite films are p and n self-doped, respectively. The carrier concentration can be tuned in a range of six orders of magnitude.[13] The p- or n-type $ASnI_3$ semiconductors are also obtained by controlling the doping levels within the Sn-based materials.[25]

The simulation of carrier concentration control is implemented to clarify the influence of the doping concentration on the performance of the p–i–n all-perovskite solar cell. Figure 2 shows the variations of the performance parameters (J_{sc}, V_{oc}, FF, E_{ff}) with doner concentration N_D in the n layer (or acceptor concentration N_A in the p layer) ranging from 10^{13} cm^{-3} to 10^{19} cm^{-3} and constant value 1×10^{18} cm^{-3} of N_A (N_D). All the performance parameters vary in a better direction with N_D and N_A increasing from 10^{13} cm^{-3} to 10^{19} cm^{-3}. When the N_D and N_A both reach 10^{19} cm^{-3}, the PCE of the solar cell is 18.38% and larger than the initial 17.20% with the N_D and N_A both kept at 10^{18} cm^{-3}.

Figure 3 shows the variations of band diagrams of the p–i–n peroskite solar cells with doping concentration of the n- and p-layers (N_D and N_A) both changing from 10^{13} cm^{-3} to 10^{19} cm^{-3}. The electric potential between n and p layers is enhanced with the increase of doping concentration. This enhanced electric field can further prompt the separation of the photon-generated carriers, reduce the recombination rate (see lines 1 and 2 in Fig. 4), and then improve the cell performance. However too high a doping concentration would cause higher recombination, and the semiconductive conductivity behavior of the perovskite would change into metallic conducting behavior. All these are harmful to the carrier transportation and then the solar cell performance.[26] Figure 5 shows the current density voltage curves with and without doping concentration optimizations of the n- and p-layer perovskite (see lines 1 and 2 in Fig. 5). Slight improvements of the cell performance with the J_{sc} of 21.58 mA/cm^2, V_{oc} of 1.07 V, FF of 81.29%, and PCE of 18.69% are obtained (see Table 2).

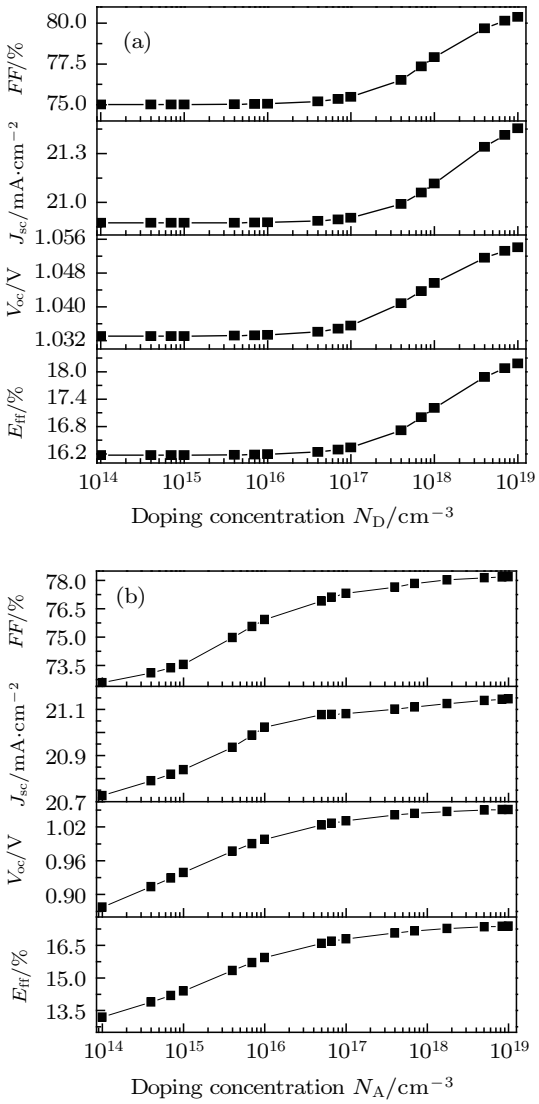


Fig. 2. Variations of the cell performance with N_D (a) and N_A (b).

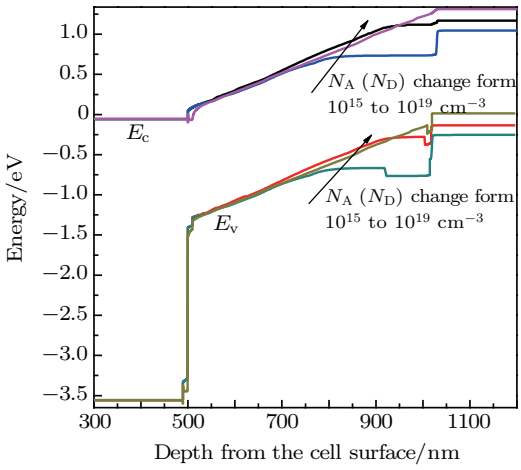


Fig. 3. (color online) Variations of the band diagrams with different doping concentrations (10^{15} cm^{-3}, 10^{17} cm^{-3}, and 10^{19} cm^{-3}) of perovskite solar cells of the n-/p-layer.

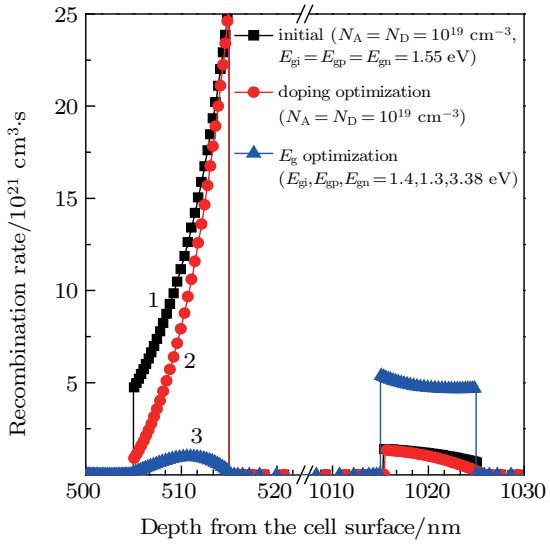


Fig. 4. (color online) Variations of the recombination rate during optimization.

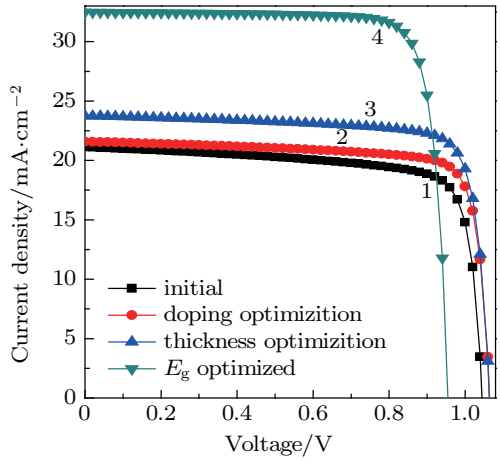


Fig. 5. (color online) Vatiations of *I*–*V* curves during optimization.

3.2. Influence of perovskite thickness

For the conventional PSCs, the main roles of the HTM and ETM (n and p layers) are to provide built-in electric field and make carriers move to the electrode effectively. The i layer is the main photon absorber and generates carriers. For our novel all-perovskite p–i–n cell, besides the charges transfer, the n and p layers also bring on light absorbing. The perovskite solar cell with double light absorbers (FTO/ZnO/$MAPbI_3$/$MAPbBr_3$/CuSCN/Au) has been first designed by Zhang *et al.*[27] The thickness of each layer in the PSC would influence the carrier production, transportation, and then have an effect on the device performance.

First, the variations of the PSC performance with the absorber layer thickness from 100 nm to 1000 nm are examined, with the thickness values fixed at 100 nm and 10 nm for the p and n layers, respectively. With the increase of the i-layer thickness, J_{sc} and V_{oc} first increase rapidly, then J_{sc} grows slowly to a saturation value and V_{oc} drops when the thickness exceeds 500 nm (see Fig. 6(a)). The *PCE* of the cells reaches a maximum value when the thickness of the i-layer is almost 500 nm. Besides absorbing more photons, the thicker absorber can induce longer transfer route of the photon-generated carriers of photons, which causes higher recombination. So an appropriate thickness of the absorber is needed for the good cell performance. The i-layer thickness is set to be an optimized value of 500 nm in the following explorations of the influences of the n- and p-layer thickness.

The variations of photoelectric property with n layer thickness in a range from 1 nm to 100 nm are shown in Fig. 6(b). The thickness values of the p layer and i layer are set to be 100 nm and 500 nm, respectively. When the n-layer thickness increases from 1 nm to 100 nm, the cell efficiency and other photovoltaic parameters decrease. So it is beneficial to reduce the n-layer thickness appropriately for the good *PCE*. The simulation shows that the closer to the surface the i layer, the more conducive to the absorbing of sunlight the i layer is. The thickness of n layer cannot be reduced unlimitedly to zero, otherwise this p–i–n structure would turn into a Schottky barrier structure, which is not good for collecting the carriers. Taking into account the preparation processes, we set 5 nm as the optimized value of the the n-layer thickness.

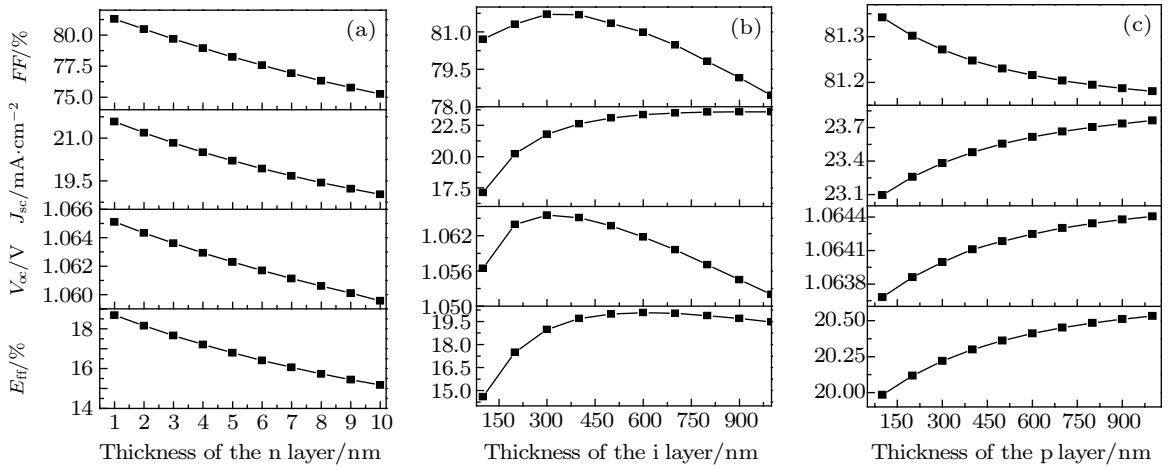


Fig. 6. Variations of cell performance with layer thickness in the p–i–n-type PSC.

Analogously, we discuss the influence of the p-layer thickness on device (see Fig. 6(c)). Let p layer increase from 100 nm to 1000 nm, then the optimized i- and n-layer thickness values will be 5 nm and 500 nm, respectively. Because of the carrier diffusion length in the PSC is on the order of 1 μm, we do not set the p layer to be thicker than 1 μm. With p-layer thickness increasing, J_{sc}, V_{oc}, and *PCE* gradually increase, while the *FF* is degraded because the series resistance increases with the increase of the p-layer thickness. The *PCE* of the solar cells almost reaches a maximum at p-layer thickness of 1000 nm.

3.3. Influence of band gap of perovskite

Experiments show that the band gap of the halide perovskites can be adjusted in a range between 1.17 eV and 4.09 eV by tailoring their inorganic and organic components.[28–32] None of the band gaps of the $CH_3NH_3Sn_{1-x}Pb_xI_3$ compounds do not follow the Vegard's law (two extremes of 1.55 eV and 1.35 eV, respectively), but each of them has a narrower band gap of 1.17 eV.[30] The experimental optical band gap of the $TMAPbBr_3$ (TMA = trimethylammonium cation) is 3.45 eV,[31] which is higher than that of the $CH_3NH_3PbCl_3$ (3.0 eV).[28] Calculation shows that the band gaps of the $Cs_2AX'_2X_4$ (A = Ge, Sn, Pb; X', X = Cl, Br, I) can change form 0.49 eV to 4.09 eV.[32] In the paper by Albrecht *et al.*, they first simulated the perovskite/c-Si tandem cells with different perovskite band gaps, and showed the optimized band gap of the perovskites that yields the highest device efficiency.[33] A $MAPbBr_3$ (E_g = 2.25 eV) –$MAPbI_3$ (E_g = 1.55 eV) tandem solar cell has been also fabricated with a high V_{oc} of 2.2 eV.[34]

In the conventional PSC, the band gap of the perovskite absorber has a significant influence on optical absorption of the cell. While for the all-perovskites solar cell, the HTM and ETM layer made of perovskite material also absorb the light. The band matchings of the p, i, n layers of the all-perovskites would benefit the improvement of the cell efficiency. The E_g influences of n and p layer on battery properties are discussed based on the former optimized doping concentration and layer thickness. The cell performance changing with the band gap of the layers is shown in Fig. 7. During the E_g of n layer increasing from 1.55 eV to 3.2 eV, the performance is improved gradually and then saturated at about 3.3 eV (see Fig. 7(a)). The high n-layer band gap can promote the short wave absorption and cut the thermalization losses caused by absorbing higher energy photons through using the next absorber with small band gap energy. The V_{oc} increases with the increase of the i-layer band gap, while the J_{sc} decreases because less and less photons can be absorbed. When the i-layer band gap is about 1.4 eV, the efficiency reaches a peak. A similar trend is found for the influence of the p-layer gap on the cell performance, and the a maximal efficiency of about 1.35 eV can be obtained.

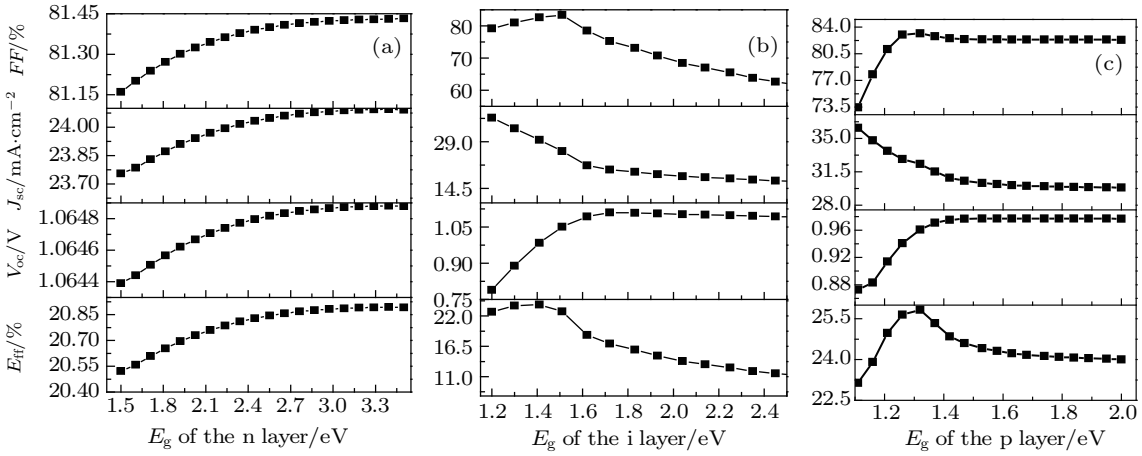


Fig. 7. Variations of cell performance with the band gap of the layer in the p–i–n type PSC.

Figure 8 shows the influences of the band matching of the i and p layer on the cell performance when the band gap of the n layer is set to be the optimized value 3.38 eV. These plots illustrate some important results. First, the i layer plays a leading role in influencing the V_{oc}, and the higher the band gap of the i layer, the higher the obtainable V_{oc} is. Second, with i-layer band gap increasing the J_{sc} decreases because of the reduction of the optical absorption of the photons with lower energy than the band gap energy. Third, the larger the difference in band gap between the i and p layers, the lower the filling factor and the efficiency of the cell are. This is because the larger gap difference can lead to the larger series resistance.

Under the condition of smaller calculating steps than the former, the best band gap matching can be obtained (see Fig. 9) with the E_g values of n-, i-, and p-layers perovskite being 3.4 eV, 1.4 eV, and 1.3 eV, respectively. It can be seen from

Fig. 5, which shows the comparison between current density–voltage curves in different optimization processes. The *I*–*V* characteristic relation of the solar cells is improved significantly after band gap has been further optimized.

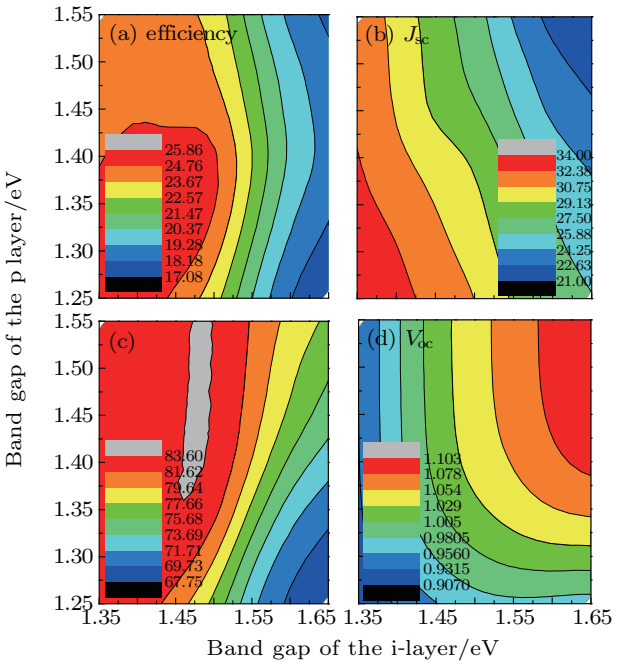


Fig. 8. (color online) Influences of the band matching of the i and p layers on the cell performance, with the band gap being 3.38 eV of the n layer.

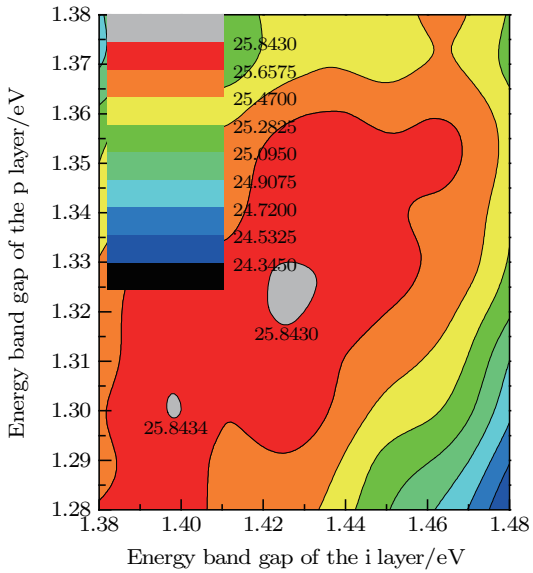


Fig. 9. (color online) Band matching under small calculating step.

After comprehensively optimizing the parameters of doping, thickness and E_g, the cell performance is significantly improved: J_{sc} reaches 32.47 mA/cm^2, V_{oc} 0.956 V, FF 83.278%, and PCE 25.843%. The cell performance is evidently increased: the efficiency is increased from an initial value of 17.05% to a final value of 25.843%, i.e., its increament reaches about 8.8%. The band matchings of the n, i, p layers dramatically expand the absorption spectrum to the larger wavelength about 980 nm and the quantum efficiency also increases at the short wavelength about 350 nm (see Fig. 10). The increase of V_{oc} is mainly due to J_{sc} significantly increasing up to about 11.3 mA/cm^2 larger than the initial value (see Table 2). The high J_{sc} is primarily driven by the widened absorption spectra (see Fig. 10) and lowered recombination rate (see line 3 in Fig. 4). The all-perovskite solar cellhas smaller series resistance than the conventional PSC, so its *I*–*V* curve near the V_{oc} is very steep (see Fig. 5).[35] The small series resistance also benefits the high J_{sc}. The using of perovskite as the carriers transporting layer and the matching of the cell energy band make a full exploration of the good charge transporting property of perovskite. All these can promote the more absorptions of the light and the lower recombination, so we obtain high short circuit current J_{sc} in the p–i–n-type all-perovskite solar cell.

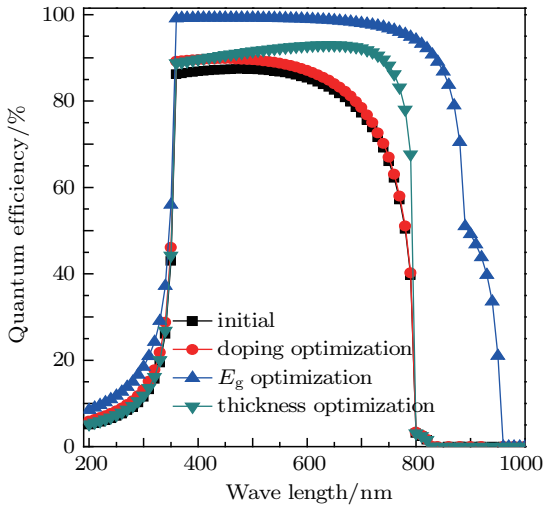


Fig. 10. (color online) Plots of quantum efficieny versus wavelength during optimization.

Yet to date, there has been no report about the theoretical research nor experimental research of the all-perovskite solar cells, future efforts should focus on the realization of the new planar p–i–n structure PSC in experiment. Fortunately, the successful fabrication of the $MAPbBr_3$–$MAPbI_3$ perovskite–perovskite tandem solar cell by simple lamination gives us some useful inspirations on the preparation process. Nonsolvent dripping, spray coating, evaporation process or inserting insoluble layer between the function layers of the all-pervoskite solar cell would avoid solving the pervoskite layers during the cell fabrication. Some insoluble materials, such as graphene oxide[36] and PTPTB[37] are used in the photoelectric devices, especially in the tandem polymer solar cell. Two-step scheme employed cross linking of the polymer is used to form the insoluble and thermally stable contact layer in the perovskite solar cells.[38,39] In our next paper, we will focus on the influence of the insoluble layer inserting on the cell performance.

4. Conclusions

A new kind of p–i–n-type all-perovskite solar cell with planar structure is designed and analyzed by using one-dimensional device simulator. The influences of the doping concentration, the band gap width and the thickness of n, i, and p layers on the performances of the solar cells are investigated. The results reveal that the n- and p-layer perovskite can work well both as transporting layer and as absorber layer. The adjustment of the band matching of the i and p layers can influence the J_{sc} and the V_{oc}, which can guide the future design of the tandem solar cell to achieve current match or high V_{oc}. The band matched cell shows obviously improved performance with widened absorption spectra and lowered recombination rate. After comprehensively optimizing the parameters mentioned above, the cell can obtain the encouraging results: the J_{sc} reaches 32.47 mA/cm^2, V_{oc} 0.956 V, FF 83.278%, and PCE 25.843%. The results are conducive to designing simpler and more efficient new perovskite cell structure in the future.

References

[1] Kojima A, Teshima K, Shirai Y and Miyasaka T 2009 *J. Am. Chem. Soc.* **131** 6050
[2] NREL chart 2016 http://www.nrel.gov/ncpv/images/efficiency_chart.jpg
[3] Mahmood K, Swain B S and Jung H S 2014 *Nanoscale* **6** 9127
[4] Lv S, Han L, Xiao J, Zhu L, Shi J, Wei H, Xu Y, Dong J, Xu X, Li D, Luo Y, Meng Q and Li X 2014 *Chem. Commun.* **50** 6931
[5] Qin P, Tanaka S, Ito S, Tetreault N, Manabe K, Nishino H, Nazeeruddin M K and Grätzel M 2014 *Nat. Commun.* **5** 3834
[6] You J, Hong Z, Yang Y M, Chen Q, Cai M, Song T B, Chen C C, Lu S, Liu Y, Zhou H and Yang Y 2014 *ACS Nano* **8** 1674
[7] Baikie T, Fang Y, Kadro J M, Schreyer M, Wei F, Mhaisalkar S G, Graetzel M and White T J 2013 *J. Mater. Chem. A* **1** 5628
[8] Stranks S D, Eperon G E, Grancini G, Menelaou C, Alcocer M J P, Leijtens T, Herz L M, Petrozza A and Snaith H J 2013 *Science* **342** 341
[9] Zhao Y, Nardes A M and Kai Z. 2014 *J. Phys. Chem. Lett.* **5** 490
[10] Heo J H, Im S H, Noh J H, Mandal T N, Lim C S, Chang J A, Lee Y H, Kim H J, Sarkar A, NazeeruddinMd K, Gratzel M and Seok S I 2013 *Nat. Photon.* **7** 486
[11] Xing G, Mathews N, Sun S, Lim S S, Lam Y M, Grätzel M, Mhaisalkar S and Sum T C 2013 *Science* **342** 344
[12] Taguchi M, Yano A, Tohoda S, Matsuyama K, Nakamura Y, Nishiwaki T, Fujita K and Maruyama E 2014 *IEEE J. Photovolt.* **4** 96
[13] Wang Q, Shao Y, Xie H, Lyu L, Liu X, Gao Y and Huang J 2014 *Appl. Phys. Lett.* **105** 163508
[14] Minemoto T and Murata M 2014 *J. Appl. Phys.* **116** 054505
[15] Minemoto T and Murata M 2014 *Curr. Appl. Phys.* **14** 1428
[16] Liu F, Zhu J, Wei J, Li Y, Lv M, Yang S, Zhang B, Yao J and Dai S 2014 *Appl. Phys. Lett.* **104** 253508
[17] Du H J, Wang W C and Zhu J Z 2016 *Chin. Phys. B* **25** 108802
[18] Zhu J Z, Qi L H, Du H J and Chai Y C 2015 *Chin. Phys. B* **24** 108501
[19] Puttnins S, Hammer M S, Neerken J, Riedel I, Daume F, Rahm A, Braun A, Grundmann M and Unold T 2015 *Thin Solid Films* **582** 85
[20] Arai T, Timmerman D, Wakamatsu R, Lee D, Koizumi A and Fujiwara Y 2015 *J. Lumin.* **158** 70
[21] Liu D and Kelly T L 2014 *Nat. Photon.* **8** 133
[22] Liu M, Johnston M B and Snaith H J 2013 *Nature* **501** 395
[23] Xiao J Y, Shi J J, Li D M and Meng Q B 2015 *Sci. China-Chem.* **58** 1
[24] Shi D, Adinolfi V, Comin R, Yuan M, Alarousu E, Buin A, Chen Y, Hoogland S, Rothenberger A, Katsiev K, Losovyj Y, Zhang X, Dowben P A, Mohammed O F, Sargent E H and Bakr O M 2015 *Science* **347** 519
[25] Stoumpos C C, Malliakas C D and Kanatzidis M G 2013 *Inorg. Chem.* **52** 9019
[26] Du H J, Wang W C, Ma B, Long T and Zhu J Z 2015 *Mat. Sci. Semicond. Proc.* **40** 570
[27] Zhang A, Chen Y and Yan J 2016 *IEEE J. Quantum Electron.* **52** 1
[28] Noh J H, Im H S, Heo J H, Mandal T N and Seok S I 2013 *Nano Lett.* **13** 1764
[29] Eperon G E, Stranks S D, Menelaou C, Johnston M B, Herz L M and Snaith H J 2014 *Energy Environ. Sci.* **7** 982
[30] Hao F, Stoumpos C C, Robert P H Chang and Kanatzid M G 2014 *J. Am. Chem. Soc.* **136** 8094
[31] Mancini A, Quadrelli P, Amoroso G, Milanese C, Boiocchi M, Sironi A, Patrini M, Guizzetti G and Malavasi L 2016 *J. Solid State Chem.* **240** 55
[32] Wang G T, Wang D Y and Shi X B 2015 *AIP Adv.* **5** 127224
[33] Albrecht S, Saliba M, Correabaena J P, Jäger K, Korte L, Hagfeldt A, Grätzel M and Rech B 2016 *J. Opt.* **18** 064012
[34] Heo J H and Im S H 2016 *Adv. Mater.* **28** 5121
[35] Yang X Z and Yang R H 2016 *Exp. Technol. Manag.* **33** 42
[36] Skaltsas T, Tagmatarchis N and Pispas S 2015 *Curr. Org. Chem.* **9** 1
[37] Yuan J, Gu J, Shi G, Sun J X, Wang H Q and Ma W L 2016 *Sci. Rep.* **6** 26459
[38] Hu Q, Liu Y, Li Y, Ying L, Liu T H, Huang F, Wang S F, Huang W, Zhu R and Gong Q H 2015 *J. Mater. Chem. A* **3** 18483
[39] Xu J X, Voznyy O, Comin R, Gong X W, Walters G, Liu M, Kanjanaboos P, Lan X Z and Sargent E H 2016 *Adv. Mater.* **14** 2807